PRAMANA — journal of physics

Vol. 85, No. 2
August 2015
pp. 211–225

Radiochemical studies on nuclear fission at Trombay

ASOK GOSWAMI
Radiochemistry Division, Bhabha Atomic Research Centre, Mumbai 400 085, India
E-mail: agoswami@barc.gov.in

DOI: 10.1007/s12043-015-1027-3; ***e*Publication:** 30 July 2015

Abstract. Since the discovery of nuclear fission in the year 1939, both physical and radiochemical techniques have been adopted for the study of various aspects of the phenomenon. Due to the ability to separate individual elements from a complex reaction mixture with a high degree of sensitivity and selectivity, a chemist plays a significant role in the measurements of mass, charge, kinetic energy, angular momentum and angular distribution of fission products in various fissioning systems. At Trombay, a small group of radiochemists initiated the work on radiochemical studies of mass distribution in the early sixties. Since then, radiochemical investigations on various fission observables have been carried out at Trombay in n, p, α and heavy-ion-induced fissions. An attempt has been made to highlight the important findings of such studies in this paper, with an emphasis on medium energy and heavy-ion-induced fission.

Keywords. Fission; mass distribution; charge distribution; angular momentum distribution; angular distribution; neutron; proton; alpha; heavy ion; accelerator; reactor.

PACS Nos 24.75.+i; 25.70.Jj; 25.85.Ca; 25.85.Ec; 25.85.Ge

1. Introduction

Fission was discovered in the year 1939 by the celebrated German radiochemists Hahn and Strassman [1]. The ability of radiochemists to separate elements from a complex mixture with very high specificity and sensitivity led to the discovery of nuclear fission. Fission is usually considered to be the property of heavy nuclei (actinides) with the mass number greater than 230. According to the liquid drop model (LDM) proposed by Bohr and Wheeler [2], the stability of a nucleus against fission is governed by the balance of surface and Coulomb energies. All nuclei in their ground state are spherical because this is the condition of minimum surface energy. For a nucleus to undergo fission, it has to deform from its spherical shape. Fission process is thus considered as a series of changes in shape from the spherical ground state to deformed scission configuration. Potential energy change associated with the change in shape calculated using LDM, passes through a maximum, called the saddle point. Energy of the saddle point relative to the ground state is called the fission barrier. According to LDM, the fission barrier decreases

systematically with the increase in atomic number and nearly vanishes around $Z = 120$. This is supported by the systematic decrease in spontaneous fission (SF) half-lives with an increase in atomic number of the actinide elements. Thus ^{238}U ($Z = 92$) has a SF half-life of about 10^{16} years while ^{258}Fm ($Z = 100$) has an SF half-life of about $\sim$1 ms.

Both collective and intrinsic degrees of freedom play important roles in the fission process. Over the years, extensive research has been carried out on various fission observables such as mass, charge, kinetic energy and angular distribution of the fission fragments/products in low as well as medium energy fission to understand the mechanism of the fission process [3,4]. While the low-energy fission is dominated by the nuclear structure effect, medium energy fission provides information on the dilution of shell effect with increasing excitation energy which is reflected in the nature of change in mass, charge and angular distributions. With the advent of heavy-ion accelerators providing heavy-ion beams over a wide range of mass and energy, it has become possible to study the fission of nuclei under extreme conditions of excitation energy, angular momentum and entrance channel mass asymmetry.

In this paper, an effort will be made to give a brief description of the radiochemical studies carried out in the Radiochemistry Division, BARC on low energy, medium energy as well as heavy-ion-induced fission, highlighting the important findings. The main objective of these studies is to understand the systematics of low-energy fission, particularly distribution of mass, charge, kinetic energy and angular momentum covering a wide range of actinide targets. The results are interpreted in terms of the spherical and deformed shells and the nucleon pairing effect. The effect of excitation energy on these distributions was studied by α-particle-induced fission. In heavy-ion-induced fission, mass, charge and angular distribution were studied to understand the role of excitation energy and angular momentum in governing the distributions. Neutron-induced fission experiments were performed at APSARA, CIRUS and DHRUVA reactors. Charged particle-induced fission experiments were carried out at Variable Energy Cyclotron Centre, Kolkata, and BARC-TIFR Pelletron-Linac Facilities. Electron beam accelerator at Khargar, Navi Mumbai was used for photon-induced fission study. The subject was reviewed in earlier articles [5–8]. In this paper the emphasis will be on the heavy-ion-induced fission.

2. Mass distribution

Mass yield distributions in neutron-induced fission of several actinides ranging from ^{227}Ac to ^{245}Cm were determined by radiochemical methods which involved separation of the fission products, followed by their estimation by β or γ counting. Absolute, relative and comparative methods [9] were used to obtain the mass distributions. Recoil catcher technique involving the collection of the recoiling fission products in a catcher foil, followed by direct γ counting using high resolution Ge(Li) detector was also used to determine the yields without chemical separation of the fission products.

The constancy of the most probable mass of the heavy wing at $A \sim 140$ and systematic increase in the most probable mass of the light wing of the mass distribution with increase in mass of the fissioning nucleus was the general trend observed [5]. The results have been attributed to the effect of $N = 82$ spherical and $N = 88$ deformed neutron shells in the heavy fragment which minimizes the potential at scission configuration [10]. Also,

the appearance of a third peak in the mass distribution of ^{228}Ac, ^{229,233}Th and ^{232}U was observed [11–13]. This has been attributed to the change in the nature of potential energy surface around the fissioning nucleus mass of about 230. It was thus concluded that the symmetric and asymmetric modes of fission are governed by the potential energy of the fissioning nucleus at the saddle point [14–16].

New experimental data were obtained on the yields of several fission products in highly asymmetric mass region in the reactor neutron-induced fission of ^{238}U. Stringent radiochemical separations were needed as the yields of the products were very low. The yields showed a shoulder in the very asymmetric region indicating the effect of 28 proton shells in the distribution [17]. Measurement of absolute fission yields in the fast neutron-induced fission of actinides, ^{238}U, ^{237}Np, ^{238}Pu, ^{240}Pu, ^{243}Am and ^{244}Cm, by track-etch-cum-gamma spectrometry were carried out [18]. The results provided new data on mass yields of several fission products. Mass distribution measurements were carried out in α-particle and proton-induced fission on ^{232}Th [19–21] to study the effect of excitation energy on mass distribution. In general, peak-to-valley (P/V) ratio has been found to decrease with increase in excitation energy of the fissioning nucleus. Also a third peak has been found to appear at symmetry. This is shown in figure 1 for ^{232}Th(p, f). The peak at the symmetry may be an indication of the effect of LDM as the shell effect tends to disappear at higher excitation energies [22].

Mass distribution studies for the ^{19}F + ^{197}Au, ^{20}Ne + ^{181}Ta, ^{20}Ne + ^{208}Pb, ^{7}Li + ^{232}Th, ^{19}F + ^{232}Th, ^{20}Ne + ^{232}Th systems were carried out using the recoil catcher technique followed by the γ-ray spectrometry [23–29]. The objective of such studies is to understand the effect of entrance channel parameters, viz., mass asymmetry, projectile energy and angular momentum on mass distribution. The mass distributions in the ^{7}Li + ^{232}Th system [25] are shown in figure 2. The asymmetric mass distributions in the beam energy range

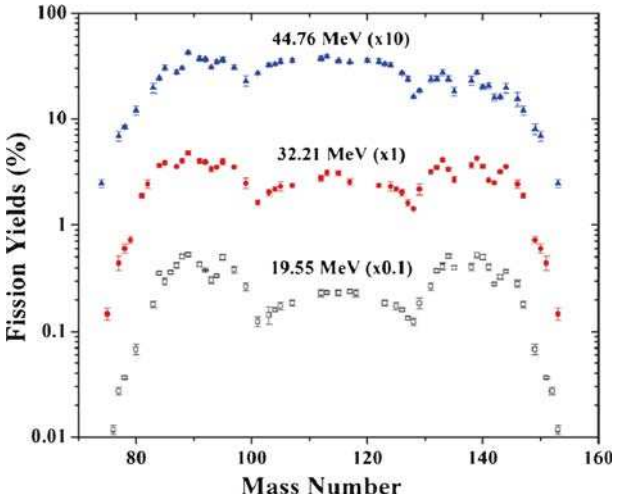

Figure 1. Yields of fission products (%) as a function of mass number in 19.5, 32.21, and 44.76 MeV proton-induced fission of ^{232}Th. Fission yields for each energy is multiplied by the number shown in brackets [21].

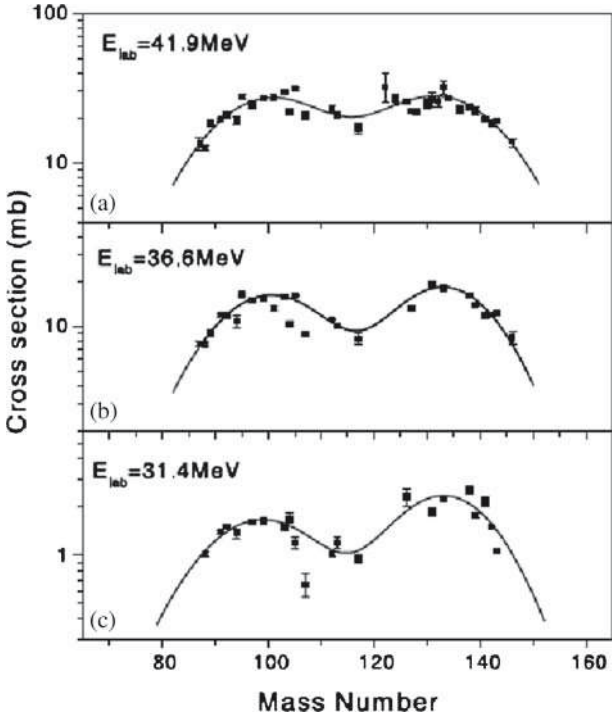

Figure 2. Mass distributions in ^{7}Li-induced fission of ^{232}Th at three beam energies. Solid lines represent the fitted curves [25].

studied indicate that the shell effect persists at these excitation energies of the compound nucleus. No significant effect of transfer-induced fission was observed in the distribution. The mass distributions for other systems studied showed broad, symmetric mass distribution indicating the disappearance of shell effect. Figure 3 shows the symmetric mass distributions in the ^{20}Ne $+^{181}$Ta system producing ^{201}Bi compound nucleus at $E_{\rm lab} = 150$ and 180 MeV [28]. An attempt was made to reproduce the observed mass distributions using the random neck rapture model (RNRM) of Brosa [30] for the ^{19}F $+^{197}$Au system producing the compound nucleus ^{216}Ra [27]. Figure 4 shows the pre-scission shape of ^{216}Ra obtained using RNRM. Analysis of the width of the symmetric mass distributions was carried out to understand the dependence of the stiffness to mass asymmetric distortion on the fissility parameter (Z^2/A) [26]. Figure 5 shows the variation. It is seen that the reduced width passes through a minimum at around the lead region, indicating that the stiffness to mass asymmetric distortion decreases on either side of lead. Also, it is seen from figure 5b that there is considerable reduction of scatter in the plot if the angular momentum-corrected fissility parameter $(Z^2/A)_{\rm eff}$ is used. This shows that the angular momentum of the fissioning nucleus increases the width of the mass distribution.

Transfer-induced fission contributes significantly to the fission cross-section for the heavy fissioning systems. Deciphering the contribution of transfer-induced fission in mass distribution was carried out for ^{19}F $+^{232}$Th, ^{11}B$+^{232}$Th and ^{20}Ne $+^{232}$Th systems [23,24,29]. Mass distributions of fission product obtained on using parameters appropriate

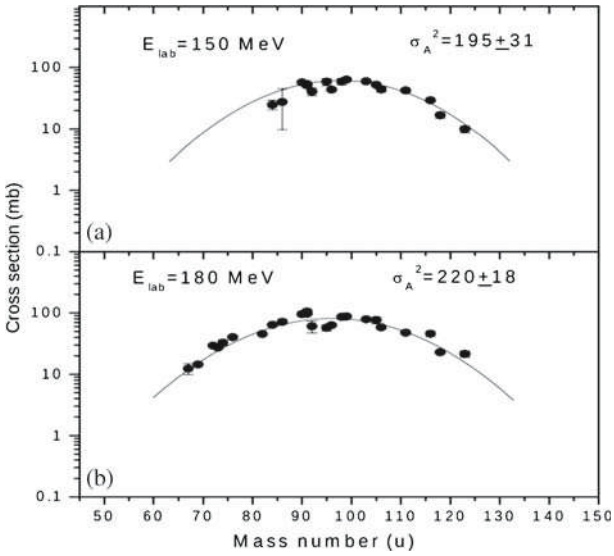

Figure 3. Mass distribution of the fission products formed in ^{20}Ne+^{181}Ta reaction at (**a**) $E_{\rm lab} = 150$ and (**b**) 180 MeV [28].

for charge distribution correction for complete fusion fission (CFF) and transfer-induced fission (TF) are shown in figure 6 for ^{20}Ne +^{232}Th system at $E_{\rm lab} = 142.5$ MeV [29]. As expected, mass distribution is symmetric for CFF indicating the absence of shell effects due to higher excitation energy of the fissioning nucleus. Mass distribution for TF has been observed to be asymmetric due to the lower excitation energy of the fissioning system. An estimate of the transfer fission cross-section has been obtained which is $\sim$15% of the total fission cross-section at this beam energy.

Mass distribution studies have been carried out in the bremsstrahlung photon-induced fission of ^{232}Th, ^{238}U, ^{240}Pu [31]. From this mass yield distribution, P/V ratios were

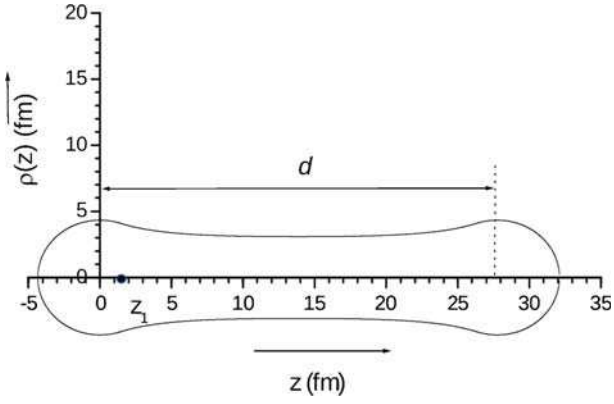

Figure 4. Pre-scission shape of ^{216}Ra [27].

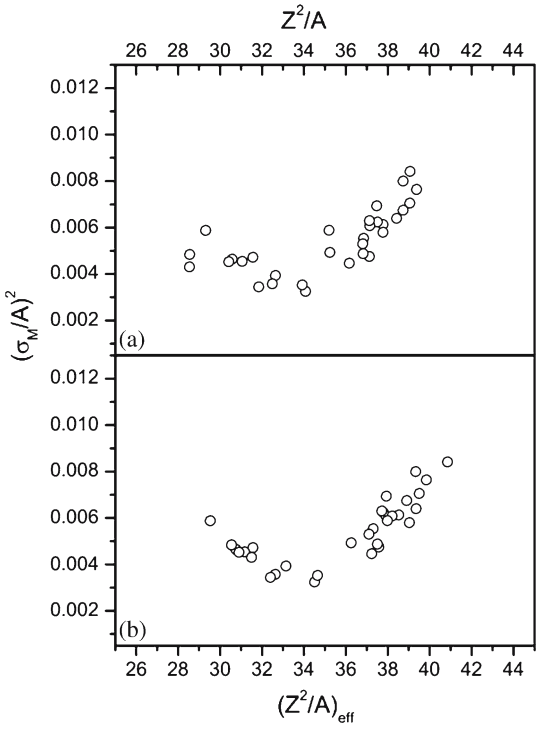

Figure 5. Plot of relative variance (**a**) $(\sigma_M/A)^2$ vs. Z^2/A and (**b**) $(\sigma_M/A)^2$ vs. $(Z^2/A)_{\text{eff}}$ [26].

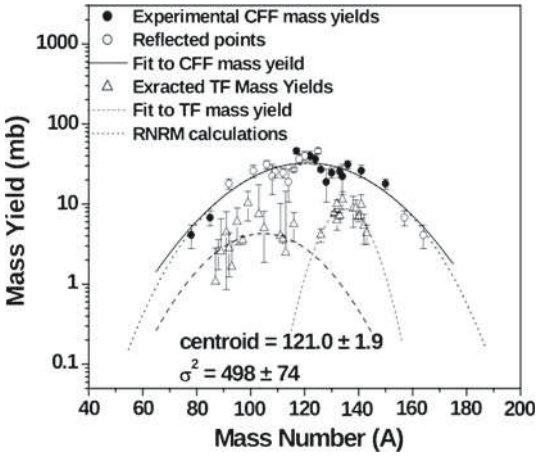

Figure 6. Mass yields for ^{20}Ne+^{232}Th reaction at $E_{\text{lab}} = 142.5$ MeV. (•) experimental CFF mass yields, (△) extracted TF mass yields, (○) reflected complementary yields, (—) the Gaussian fit to the yields for CFF, (· · · · ·) the RNRM calculations and (- - - - -) the Gaussian fit to TF mass yields [29].

obtained. The results along with the data of neutron-induced fission were used to obtain the excitation energy dependence of P/V ratio.

3. Charge distribution studies in fission

The charge distribution study provides information on the distribution of nuclear charge between two complementary fragments of fixed masses. The study involves the measurement of independent yields of members of isobaric chain or isotopes of an element. The charge distribution in fission is assumed to be Gaussian characterized by two parameters: mean or the most probable charge Z_{p} and the variance σ_z^2. The corresponding parameters for isotopic yield distribution are A_{p} and σ_A^2. Nuclear structure as well as excitation energy govern these parameters for different fissioning systems. The charge distribution parameters also provide information on N/Z equilibration and dynamics of descent from saddle to scission. Radiochemical method involves the separation of the individual members of the isobaric chain and determination of their yields. A detailed compilation of the independent yields and the charge distribution parameters for neutron-induced fission and SF are available in ref. [32]. In Radiochemistry Division, independent and cumulative yields of several fission products in neutron-induced fission of several actinide targets ranging from ^{229}Th to ^{245}Cm and SF of ^{252}Cf were carried out to obtain information of nuclear shell and pairing effects on the distribution. In one of the experiments a 6 μg ^{252}Cf source was used for charge distribution studies. The values of Z_{p} were obtained for several mass chains and the corresponding charge polarization parameters $Z_{\mathrm{p}} - Z_{\mathrm{UCD}}$ (ΔZ) were calculated where Z_{UCD} corresponds to the unchanged charge distribution [7]. It was seen that the charge polarization increases with mass asymmetry.

Charge distribution studies were also carried out with other fissioning systems to obtain Z_p and σ_z^2 for different fragment masses [33]. These data along with the literature-reported values were analysed to obtain information on nuclear shell and pairing effect on charge distributions in ^{233}Th, ^{233}U, ^{234}U, ^{236}U, ^{239}Pu, ^{240}Pu and ^{246}Cm. The odd–even effect was found to decrease with the increase in mass of fissioning nucleus and the results were consistent with the data in [32]. Similar to isobaric yield distribution, isotopic yield distributions have also been determined for different fissioning systems in low and heavy-ion-induced fission. The values of A_{p}, σ_A and charge yield can be extracted from such distributions. The comparison of charge yield of Tc in ^{233}U(n, f), ^{239}Pu(n, f) and ^{252}Cf(SF) showed the effect of 82 spherical and deformed 88 neutron shells in the complementary heavy fission fragment, in enhancing the charge yield of Tc from ^{233}U(n, f) to ^{252}Cf(SF) [34].

Both isotopic and isobaric charge yield distributions were studied in heavy-ion-induced fission [26,28,29] to obtain information about the charge distribution parameters at higher excitation energy. Broadening of the charge distribution compared to low-energy fission and absence of shell effect are the two characteristics of medium energy and heavy-ion-induced fission [35–38]. Figure 7 shows the Gaussian isotopic yield distribution of Sb isotopes in the ^{20}Ne $+^{232}$Th fissioning system [29]. In heavy-ion-induced fission of actinide targets, as stated earlier, TF can constitute a significant fraction of the fission cross-section. Charge distribution studies provide information on the TF in heavy-ion-induced fission. A plot of independent or nearly independent (fission products at the lower

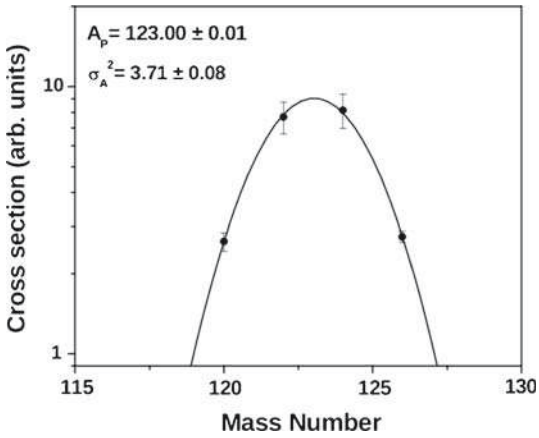

Figure 7. Plot of yields of Sb isotopes in the forward catcher foil at $E_{\text{lab}} = 142.5$ MeV for $^{20}\text{Ne} + ^{232}\text{Th}$ reaction. Solid line is Gaussian fit to the data. Variance and most probable mass obtained from the fit are also shown in the figure. The quoted uncertainty is the fitting error [29].

end of the isobaric yield distribution) yields of fission products as a function of their A/Z show two separate groups of fission products arising from the CFF (centred at lower A/Z) and TF (centred at higher A/Z) which differ in their most probable charge-to-mass ratio [23,29]. This has been used to obtain information about the contribution of TF in reactions involving actinide targets.

4. Angular momentum distribution of fission fragments

The fission fragments in low-energy fission possess angular momentum which far exceeds the value expected from the spin of the compound nucleus. The mechanism of generation of angular momentum in the fission fragment is an interesting topic of research. It is believed to arise from the nonlinear scission configuration and post-scission Coulomb torque [39–41]. Both physical [42] and radiochemical methods were used to obtain information about the fragment angular momentum.

Isomeric yield ratios (IYR) of the fission products having low and high spin isomers provide information about the corresponding fragment angular momentum. A statistical model is used to calculate the fragment de-excitation by neutron and γ emission, leading to the population of high and low spin states of the fission product. The IYR of isotopes of Nb, Pd, Cd, Sb, Te and I were determined radiochemically for several fissioning systems, both in neutron- and α-induced fission [43–49]. The results were interpreted in terms of fragment shell and pairing effect, input excitation energy and angular momentum. It was shown that the odd-Z fragments have higher angular momentum compared to the even-Z fragment and was shown to have inverse correlation with the yields of odd-Z and even-Z fission products in ^{252}Cf(SF). Figure 8 shows the odd–even fluctuation in charge yields and fragment angular momentum [45]. It was shown that the angular momenta decrease as the neutron number in the fragments approaches 82 spherical neutron shell [45,48]. The results show that the fragment angular momenta increase with deformation.

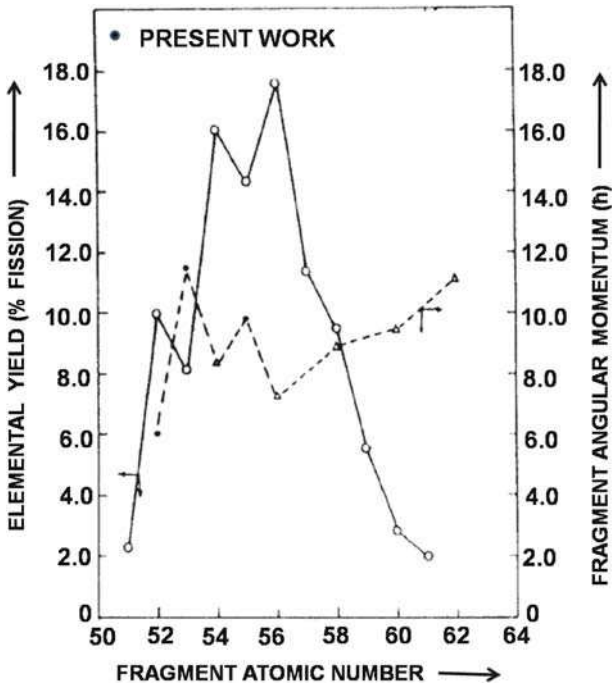

Figure 8. Correlation of the elemental yield and angular momentum in ^{252}Cf(SF) [45].

The effect of initial excitation energy and angular momentum on the fragment angular momentum was studied in α-particle-induced fission of ^{232}Th and ^{238}U [44,46–48]. Figure 9 shows the variation of fragment angular momentum of the ^{126,128,130}Sb isotopes with the initial excitation energy of the fissioning nucleus in ^{238}U(α, f) [48]. With the increase in excitation energy of the fissioning nucleus, the excitation energy of the fragment also increases, allowing thermal accessibility of higher angular momentum states. Thus, the fragment angular momentum increases. Also, the values are lowest for the isotope 130 which is in close proximity with the spherical 82 neutron shell which shows fragment deformation and plays an important role in governing the fragment angular momentum.

5. Mass-resolved angular distribution of fission fragments

Angular distribution of fission fragments reflects the saddle point states (J, K) through which the fissioning nucleus passes during its motion towards scission [50]. For fission at an excitation energy well above the barrier, the statistical saddle point model is used to explain the angular distribution of fission fragments [51]. According to this model, angular distribution is governed by the angular momentum of the entrance channel, excitation energy and the shape of the fissioning nucleus at saddle. Angular distribution of fission fragments were extensively studied for both neutron and charged particle-induced fission using physical methods [3,52–54].

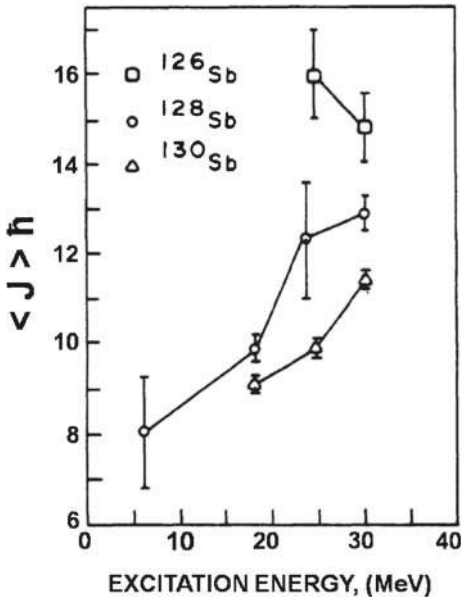

Figure 9. Variation of fragment angular momentum ($\langle J \rangle$) with excitation energy of the fissioning nucleus [48].

In order to investigate the correlation between mass and angular distributions, mass-resolved angular distribution was studied in Radiochemistry Division using recoil catcher technique for several fissioning systems in both α-particle and heavy-ion-induced fission. The fragments were collected at different angles using a cylindrical irradiation chamber. From the end of irradiation activity (A_i) in different strips, the laboratory angular distribution of a given fission product was obtained. In general, angular anisotropy ($W(0°)/W(90°)$) is found to increase with mass asymmetry for proton and α-induced fission of Th–Pu targets [3,55,57]. Figure 10 shows the plot of angular distribution of some fission products, representing symmetric and asymmetric fission in the ^{4}He $+^{232}$Th system [57]. The values of angular anisotropies can be seen within the figure. The asymmetric fission products show higher anisotropy compared to the symmetric fission products. Though the results indicate that angular anisotropies are related to mass asymmetry, the interpretation is not unambiguous as multichance fission can influence the results. In order to see the effect of the entrance channel mass asymmetry, mass-resolved angular distribution was determined in ^{4}He $+^{240}$Pu and $p+^{243}$Am systems, both producing the same compound nucleus ^{244}Cm at about the same excitation energy. Figure 11 shows the plot of angular anisotropies vs. mass number of different fission products in the two systems. It is seen that the angular anisotropy is independent of mass asymmetry in both the systems. However, the effect of the entrance channel is visible on the average anisotropy which is higher in the ^{4}He $+^{240}$Pu system. This is due to the higher angular momentum of the entrance channel brought in by helium ion compared to the proton. Also, due to the odd mass number of p and ^{243}Am, the entrance channel spin is not zero in this system which results in reduced anisotropy.

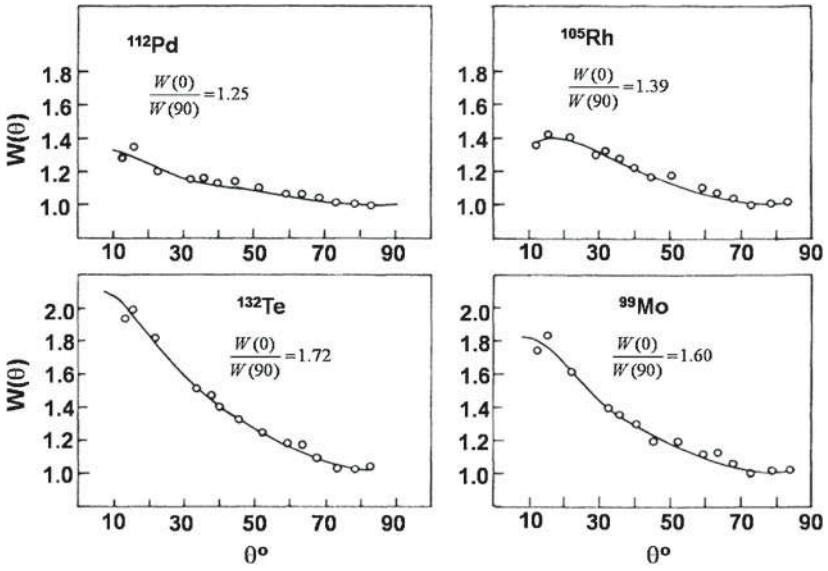

Figure 10. Experimental angular distributions for symmetric and asymmetric products in helium ion-induced fission of ^{232}Th [57].

In heavy-ion induced fission, ^{12}C+^{232}Th, ^{11}B+^{232}Th systems do not show any mass dependence of angular anisotropy while ^{16}O+^{232}Th systems shows higher anisotropies for the symmetric fission products [58]. The trend is thus reversed compared to the light ion-induced fission. Mass-resolved angular distribution studies were also carried out in the ^{20}Ne+^{181}Ta [28], ^{20}Ne+^{208}Pb [26] and ^{20}Ne+^{232}Th [59] systems. It is observed that the angular anisotropy is not correlated with the mass asymmetry in the ^{20}Ne+^{181}Ta and

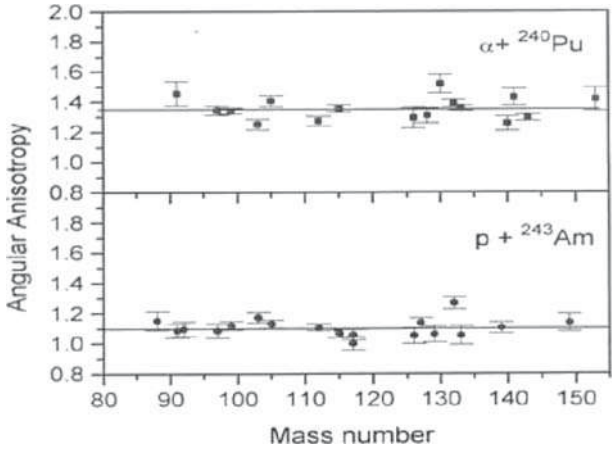

Figure 11. Angular anisotropy vs. mass number for ^{244}Cm CN formed by two different entrance channels (Goswami *et al* [56]).

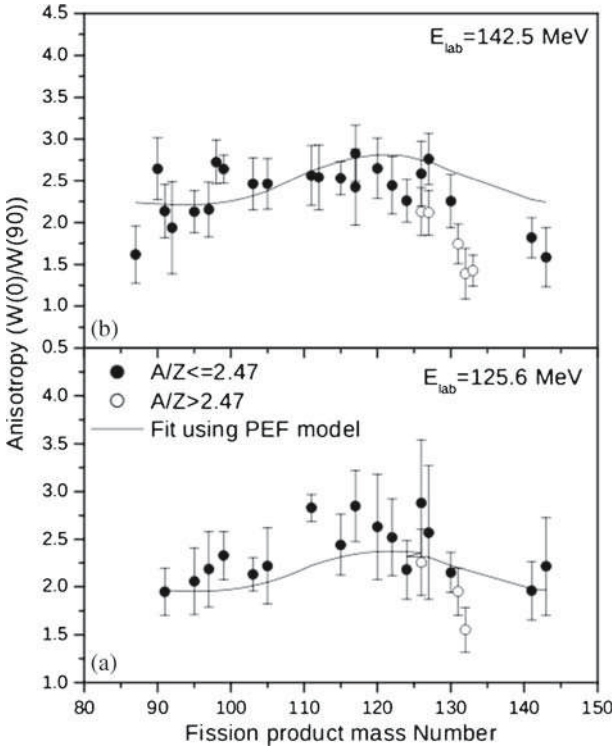

Figure 12. Angular anisotropies of various fission products formed in ^{20}Ne+^{232}Th reaction at (**a**) $E_{\rm lab} = 125.6$ MeV and (**b**) $E_{\rm lab} = 142.5$ MeV. Filled and open circles represent the fission products with $A/Z \leq 2.47$ and $A/Z > 2.47$, respectively. Solid lines are fit to experimental anisotropies using pre-equilibrium fission [59].

^{20}Ne+^{208}Pb systems. At higher excitation energies and angular momentum of the compound nucleus, many deviations from the statistical theory are reported [60,61]. The ^{20}Ne+^{232}Th system also shows higher anisotropy for symmetric fission products like ^{16}O+^{232}Th, as shown in figure 12. The increase in angular anisotropy indicates the contribution from pre-equilibrium fission, in which fission occurs before the complete equilibration of K-degree of freedom. The experimental trend of anisotropies can be explained qualitatively after including the contribution from pre-equilibrium fission as shown by the solid lines in figure 12. Such a mass dependence of angular anisotropy may be a feature specific to pre-equilibrium fission and, therefore, may be used to distinguish from quasi-fission, in which, fissioning systems escape into the exit channel without being captured inside the saddle point.

6. Conclusion

Radiochemical studies on charge, mass and angular distributions of fission products have been used to gain insight into low energy and heavy-ion-induced fission process. The data on the variance of mass distribution provide information about the stiffness

of the potential energy surface to mass asymmetric deformations. Substantial contribution from transfer-induced fission has been observed in highly fissile system which was distinguished based on the A/Z of the fission products. Mass-resolved angular distributions of fission products gave information about the saddle-to-scission dynamics as well as about the contribution from non-equilibrium fission processes owing to the entrance channel dynamics. Mass-resolved angular distribution of fission products provides a possibility to distinguish between pre-equilibrium fission and fusion–fission process. More studies on this aspect will help one to understand the contributions from various non-compound nucleus fission processes in the heavy actinide and transactinide regions.

Acknowledgements

The author sincerely thanks all his colleagues of Nuclear Chemistry Section of Radiochemistry Division and Fission Physics Group of Nuclear Physics Division, who have contributed to the work presented here.

References

[1] O Hahn and F Strassman, *Naturewiss.* **11**, 27 (1939)
[2] N Bohr and J A Wheeler, *Phys. Rev.* **56**, 426 (1939)
[3] R Vandenbosch and J Huizenga, *Nucl. Fission* (Academic, New York, 1973)
[4] C Wagemans, *The nuclear fission process* (CRC, London, 1990)
[5] M V P Ramaniah, *Pramana – J. Phys.* **24**, 137 (1985)
[6] Satya Prakash, *Pramana – J. Phys.* **33**, 108 (1989)
[7] S B Manohar, A Ramaswami, B K Srivastava, A V R Reddy, A G C Nair, G K Gubbi, A Srivastava and Satya Prakash, *Nucl. Phys. A* **502**, 307c (1989)
[8] S B Manohar, B S Tomar and V K Manchanda, *J. Nucl. Radiochem. Sci.* **1(1)**, 2732 (2000)
[9] H C Jain and M V Ramaniah, *Radiochim. Acta* **19**, 90 (1973)
[10] B D Wilkins, R R Steinberg and R R Chasman, *Phys. Rev. C* **14**, 1832 (1976)
[11] R H Iyer, C K Mathews, N Ravindran, K Rengan, B D Singh, M V Ramaniah and H D Sharma, *J. Inorg. Nucl. Chem.* **25**, 465 (1963)
[12] S S Rattan, A V R Reddy, R J Singh, Satya Prakash and M V Ramaniah, *Radiochim. Acta* **33**, 189 (1983)
[13] S B Manohar, P P Venkatesan, S M Deshmukh, Satya Prakash and M V Ramaniah, *Phys. Rev. C* **19**, 1827 (1979)
[14] P Moller and S G Nilsson, *Phys. Lett. B* **31**, 283 (1970)
[15] P Moller and J R Nix, *Nucl. Phys. A* **229**, 269 (1974)
[16] D C Hoffman, *Proc. Phys. Chem. of Fission IAEA* **2**, 275 (1980)
[17] V K Rao, V K Bhargava, S G Marathe, S M Sahakundu and R H Iyer, *Phys. Rev. C* **19**, 1372 (1979)
[18] R H Iyer, H Naik, A K Pandey, P K Kalsi, R J Singh, A Ramaswami and A G C Nair, *Nucl. Sci. Eng.* **135**, 227 (2000)
[19] R Guin, S M Sahakundu, S B Manohar, Satya Prakash, M V Ramaniah, *Radiochim. Acta* **48**, 7 (1989)
[20] R Guin, S M Sahakundu, S B Manohar and Satya Prakash, *Radiochim. Acta* **48**, 7 (1989)

[21] H Naik, A Goswami, G N Kim, K Kim and S V Suryanarayana, *Eur. Phys. J. A* **49**, 133 (2013)
[22] K-H Schmidt, S Steinhaeuser, C Boeckstiegel, A Grewe, A Heinz, J Junghans, J Benlliure, H G Clerc, M de Jong, J Mueller, M Pfuetzner and B Voss, *Nucl. Phys. A* **665**, 221 (2000)
[23] G K Gubbi, A Goswami, B S Tomar, B John, A Ramaswami, A V R Reddy, P P Burte and S B Manohar, *Phys. Rev. C* **53**, 796 (1996)
[24] G K Gubbi, A Goswami, B S Tomar, B John, A Ramaswami, A V R Reddy, P P Burte and S B Manohar, *Phys. Rev. C* **59**, 3224 (1999)
[25] R Tripathi, K Sudarshan, S Sodaye, B S Tomar, G K Gubbi, A Goswami, A V R Reddy and S B Manohar, *Radiochim. Acta* **90**, 185 (2002)
[26] R Tripathi, K Sudarshan, A Goswami, P K Pujari, B S Tomar and S B Manohar, *Phys. Rev. C* **69**, 024613 (2004)
[27] R Tripathi and A Goswami, *Eur. Phys. J. A* **26**, 271 (2005)
[28] R Tripathi, K Sudarshan, A Goswami, R Guin and A V R Reddy, *Phys. Rev. C* **74**, 014610 (2006)
[29] S Sodaye, R Tripathi, K Sudarshan and R Guin, *Phys. Rev. C* **87**, 044610 (2013)
[30] U Brosa and S Grossmann, *Z. Phys. A* **310**, 177 (1983)
[31] H Naik, V T Nimje, D Raj, S V Suryanarayana, A Goswami, Sarbjit Singh, S N Acharya, K C Mittal, S Ganesan, P Chandrachoodan, V K Manchanda and S Banerjee, *Nucl. Phys. A* **853**, 1 (2011)
[32] A C Wahl, *At. Data Nucl. Data Tables* **39**, 1 (1988)
[33] H Naik, S P Dange, R J Singh and S B Manohar, *Nucl. Phys. A* **612**, 143 (1997)
[34] A Srivastava, A Goswami, B K Srivastava, A G C Nair, S B Manohar, Satya Prakash and M V Ramaniah, *Phys. Rev. C* **33(3)**, 969 (1986)
[35] H Umezawa, S Baba and H Baba, *Nucl. Phys. A* **160**, 65 (1971)
[36] J V Kratz, O Linljenzin, A E Norris and G T Seaborg, *Phys. Rev. C* **13**, 2347 (1976)
[37] M C Duh, H Haba, N Takahashi, A Yokoyama and T Saito, *Nucl. Phys. A* **550**, 281 (1992)
[38] S B Manohar, A Goswami and B S Tomar, *J. Radioanal. Nucl. Chem.* **203**, 331 (1996)
[39] J O Rasmussen, W Norenberg and H J Mang, *Nucl. Phys. A* **136**, 456 (1969)
[40] M M Hoffman, *Phys. Rev. B* **133**, 714 (1964)
[41] L G Moretto and R P Schmitt, *Phys. Rev. C* **21**, 204 (1980)
[42] J B Wilhelmy, R C Cheifetz, R C Jared, S G Thompson and J O Rasmussen, *Phys. Rev. C* **5**, 2041 (1972)
[43] T Datta, S P Dange, A G C Nair, S Prakash and M V Ramaniah, *Phys. Rev. C* **25(1)**, 358 (1982)
[44] T Datta, S M Sahakundu, S P Dange, N Chakravarty, R Guin and S Prakash, *Phys. Rev. C* **28(3)**, 1206 (1983)
[45] T Datta, S P Dange, S K Das, S Prakash and M V Ramaniah, *Z. Phys. A: Atomic Nuclei* **324(1)**, 81 (1986)
[46] T Datta, S P Dange, S M Sahakundu, S Prakash and M V Ramaniah, *Z. Phys. A: Atomic Nuclei* **330(1)**, 103 (1988)
[47] B S Tomar, A Goswami, S K Das, T Datta, B K Srivastava, A G C Nair, S Prakash and M V Ramaniah, *Z. Phys. A: Atomic Nuclei* **327(2)**, 225 (1987)
[48] B S Tomar, A Goswami, S K Das, B K Srivastava, R Guin, S M Sahakundu and S Prakash, *Phys. Rev. C* **38(4)**, 1787 (1988)
[49] H Naik, T Datta, S P Dange, P K Pujari, S Prakash and M V Ramaniah, *Z. Phys. A: Atomic Nuclei* **331(3)**, 335 (1988)
[50] A Bohr, *Proc. of the United Nations Int. Conf. on the Peaceful Uses of Atomic Energy, Geneva* (United Nations, New York, 1955) Vol. 2, p. 131

[51] I Halpern and V M Strutinsky, in: *Proceedings of the Second United Nations International Conference on Peaceful Uses of Atomic Energy, Geneva* edited by J H Martens *et al* (United Nations, Switzerland, 1958), Vol. 15, p. 408
[52] S Kailas, *Phys. Rep.* **292**, 131 (1998)
[53] S S Kapoor and V S Ramamurthy, *Pramana – J. Phys.* **33**, 161 (1989)
[54] B B Back, R R Betts, K Cassidy, B G Glagola, J E Gindler and B D Wilkins, *Phys Rev. Lett.* **50**, 818 (1983)
[55] A Goswami, S B Manohar, S K Das, A V R Reddy, B S Tomar and S Prakash, *Z. Phys. A* **342**, 299 (1992)
[56] A Goswami, B S Tomar, G K Gubbi and S B Manohar, *DAE Symposium on Nuclear Physics* (Bangalore University, Dec. 1997) p. 505
[57] T Datta, S P Dange, H Naik and S B Manohar, *Phys. Rev. C* **48**, 221 (1993)
[58] Bency John, Aruna Nijasure, S K Kataria, A Goswami, B S Tomar, A V R Reddy, S B Manohar *et al*, *Phys. Rev. C* **51**, 165 (1995)
[59] R Tripathi, S Sodaye, K Sudarshan and R Guin, *Phys. Rev. C* **88**, 24603 (2013)
[60] H Rossner, D Hilscher, E Holub, G Ingold, U Jahnke, H Orf, J R Huizenga, J R Birkelund, W U Schrüder and W W Wilcke, *Phys. Rev. C* **27**, 2666 (1983)
[61] C R Morton, A C Berriman, R D Butt, M Dasgupta, A Godley, D J Hinde and J O Newton, *Phys. Rev. C* **62**, 024607 (2000)